Optics Communications 284 (2011) 490–493

Contents lists available at ScienceDirect

Optics Communications

journal homepage: www.elsevier.com/locate/optcom

# Polarization beam splitter based on photonic crystal self-collimation Mach–Zehnder interferometer

Xiyao Chen [a,*], Zexuan Qiang [b], Deyin Zhao [c], Yufei Wang [b], Hui Li [b], Yishen Qiu [b], Weidong Zhou [c]

[a] Department of Physics and Electronic Information Engineering, Minjiang University, Fuzhou 350108, China
[b] School of Physics and Optoelectronics Technology, Fujian Normal University, Fuzhou, 350007, China
[c] Department of Electrical Engineering, NanoFAB Center, University of Texas at Arlington, Texas 76019, USA

ARTICLE INFO

*Article history:*
Received 19 June 2010
Received in revised form 27 August 2010
Accepted 31 August 2010

*Keywords:*
Photonic crystal
Self-collimation
Polarization beam splitter
Mach–Zehnder interferometer

ABSTRACT

A polarization beam splitter based on a self-collimation Mach–Zehnder interferometer (SMZI) in a hole-type silicon photonic crystal was proposed and numerically demonstrated. Utilizing polarization dependence of the transmission spectra of the SMZI and polarization peak matching (PPM) method, the SMZI can work as a polarization beam splitter (PBS) by selecting appropriate path length difference in the structure. Because of its intrinsic operating principle, the PBS possesses high polarization extinction ratios (PERs). As its dimensions are only several operating wavelengths, the PBS may have practical applications in photonic integrated circuits.



## 1. Introduction

Self-collimation (SC) effect in photonic crystal (PC) structures allows diffractionless light propagation in perfect PCs without "physical" guiding boundaries (e.g. line-defect waveguide) [1,2]. It can also enable self-collimated light beams to intercross without cross-talks like in free space. Various PC devices based on this unique phenomenon have been theoretically and experimentally demonstrated [3–13]. Among them, self-collimation Mach–Zehnder interferometers (SMZIs) can work as wavelength splitters (i.e., wavelength division demultiplexer) or power splitters [6,8,11,12]. All these PC devices work for only one polarization. Not long ago, we proposed polarization-independent drop filters based on photonic crystal self-collimation ring resonators, which utilize the common SC frequency range in a hole-type silicon photonic crystal shared by both transverse-electric (TE) and transverse-magnetic (TM) polarizations [14].

Large birefringence exists in photonic crystals because of their highly anisotropic structures. So it can be anticipated that TE and TM transmission characteristics of a SMZI are quite different even in the common SC frequency range. Utilizing this property and the polarization peak matching (PPM) technique [14], we demonstrate here that a SMZI with appropriate structure can work as a polarization beam splitter (PBS). Compared with other PBSs based on photonic crystals proposed in recent years [9,15–18], the PBS based on a SMZI has higher polarization extinction ratios (PERs) for both TE and TM modes, which results from destructive interference between self-collimated beams.

In this paper, we first describe the dispersion properties in polarization-independent self-collimation frequency range, followed by the analyses of the SMZI transmission spectra based on the theory of beam interference. Finally, we utilize the PPM method to design a SMZI-based PBS.

## 2. Polarization-independent self-collimation frequency range

Here we consider a two-dimensional (2D) photonic crystal consisting of a square lattice of air holes in silicon (Si) with the dielectric constant ε of 12, as shown in the inset of Fig. 1(c). The radius of air holes is $r = 0.33a$, where $a$ is lattice constant. Fig. 1(a) and (b) shows some equal frequency contours (EFCs) of the first photonic band in a quarter of the first Brillouin zone for TE and TM modes, respectively, all calculated by the plane-wave expansion (PWE) method. Dispersion curves along ΓM direction for two polarizations are also shown in Fig. 1(c).

The direction of the energy flow for light propagation is always perpendicular to the corresponding EFCs [19]. From Fig. 1(a) and (b), the EFCs in the frequency range between $0.176c/a$ and $0.19c/a$ for both TE and TM polarizations are close to straight lines normal to the ΓM direction (where $c$ is the speed of light in vacuum). This indicates that both TE and TM lights in that frequency range can travel without diffraction along ΓM direction in the PC, which is so-called SC effect. This common SC frequency window for both TE and TM polarizations

* Corresponding author.
*E-mail address:* chenxy2628@yahoo.com.cn (X. Chen).

0030-4018/$ – see front matter © 2010 Elsevier B.V. All rights reserved.
doi:10.1016/j.optcom.2010.08.081

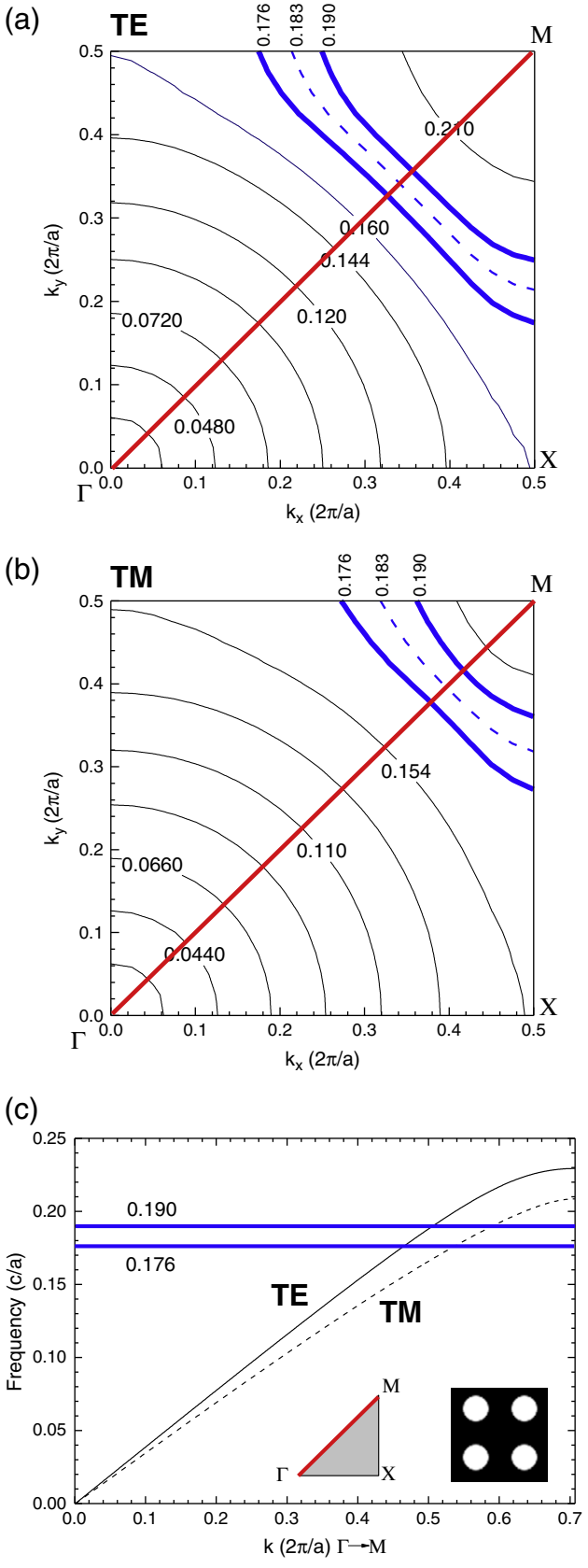


**Fig. 1.** Equal frequency contours (EFCs) of the first band for (a) TE modes and (b) TM modes in a silicon photonic crystal consisting of a square lattice of air holes. (c) Dispersion curves for two polarizations along ΓM direction. Inset: the air hole radius $r$ equals $0.33a$, where $a$ is the lattice constant. The regions between two blue solid lines correspond to the SC frequency window.

is essential in forming polarization-related photonic devices based on SC effect.

As shown in Fig. 1(c), the dispersion relations for two polarizations are different, due to the birefringence nature of the PC. Within the common SC frequency range between $0.176c/a$ and $0.19c/a$, both polarization modes have approximately linear dispersion relations:

$$f = (c/2\pi n_e)k + f_0 \tag{1}$$

where $n_e$ is the effective refractive index for SC light, $k$ is the Bloch wave-vector, and $f_0$ is a fitting parameter. Best linear fits can result in the following parameters: $n_{e,TE} = 2.8739$, $f_{0,TE} = 0.00761c/a$ for TE polarization, and $n_{e,TM} = 3.8794$, $f_{0,TM} = 0.03795c/a$ for TM polarization. It is worth noticing that significant birefringence exists with the ratio of the effective refractive indices for TE and TM modes to be $n_{e,TE} : n_{e,TM} \approx 3 : 4$.

## 3. Structure and characteristics of SMZI

The existence of the polarization-independent self-collimation frequency range makes it possible to design self-collimation filters that can be shared by two polarizations. The structure of the SMZI we proposed is shown in Fig. 2(a), which consists of two same mirrors ($M_1$ and $M_2$) and two same beam splitters ($S_1$ and $S_2$) in the photonic crystal aforementioned. Narrow-width light beams can propagate without diffraction in the SMZI in dependence on self-collimation effect. Each mirror is formed by inserting a thick air bar, overlapping five-row air holes along the ΓX direction. Each beam splitter is formed by inserting an air line with $0.41a$ width, overlapping part of one-row air holes along the ΓX direction. In the SMZI, the incident SC light beam is split by $S_1$ into two beams that travel along the upper (longer) and down (shorter) light paths, respectively. The length of the shorter path is equal to $l_1$ while the length of the longer path is equal to $l_2$. It can be seen that $l_2 = l_1 + 2d$, where $d$ represents the distance between $S_1$ and $M_1$, or between $S_2$ and $M_2$. The two SC beams from two paths are split again by $S_2$. Light interference happens at the bottom and right output ports after $S_2$.

The performance of the beam splitters was first evaluated based on the finite-difference time-domain (FDTD) simulation method, with the results shown in Fig. 2(b). It is worth noting that the reflectivity ($R_s$) and transmittivity ($T_s$) of the splitters over SC frequency range are highly polarization dependent. Both $R_{s,TM}$ and $T_{s,TM}$ are around 50% for TM polarization, while $R_{s,TE}$ is around 90% and $T_{s,TE}$ is around 10% for TE polarization. The splitters are nearly lossless because $R_s + T_s \approx 1$. In other words, the splitting ratio of the splitters is 1:1 for TM modes.

The theoretical transmission at two output ports in the SMZI can be obtained based on the theory of light interference in the following form [20]:

$$I_1 / I_0 = 4R_sT_s\cos^2[k(l_{2e} - l_1)/2] \tag{2}$$

$$I_2 / I_0 = 1 - 4R_sT_s\cos^2[k(l_{2e} - l_1)/2] \tag{3}$$

where $R_s$ and $T_s$ are the reflectivity and transmittivity of $S_1$ (or $S_2$). $I_0$ is the intensity of the input SC light, $I_1$ and $I_2$ are the intensities of the SC light at the bottom and right output ports respectively. $l_{2e}$ represents the effective length of the longer light path. Like in [14], $l_{2e} = l_1 + 2d + 2l_p$, where $l_p$ represents the penetration depth into $S_1$ (or $S_2$) when the SC beam is reflected. $l_p$ and thus $l_{2e}$ are polarization dependent. Here we assumed that each of two mirrors is perfect, with reflectivity of 100% and phase shift of π for one-time reflection [8].

From Eqs. (2) and (3), the bottom transmission ($I_1/I_0$) and right transmission ($I_2/I_0$) are complementary because $I_1 + I_2 = I_0$. They have equal amplitude of $4R_sT_s$ although the bottom transmission is in the range $[0, 4R_sT_s]$ and the right is in the range $[(1 - 4R_sT_s), 1]$. For a lossless splitter, $R_s + T_s = 1$. When $R_s = T_s = 0.5$ (i.e., $4R_sT_s = 1$), the

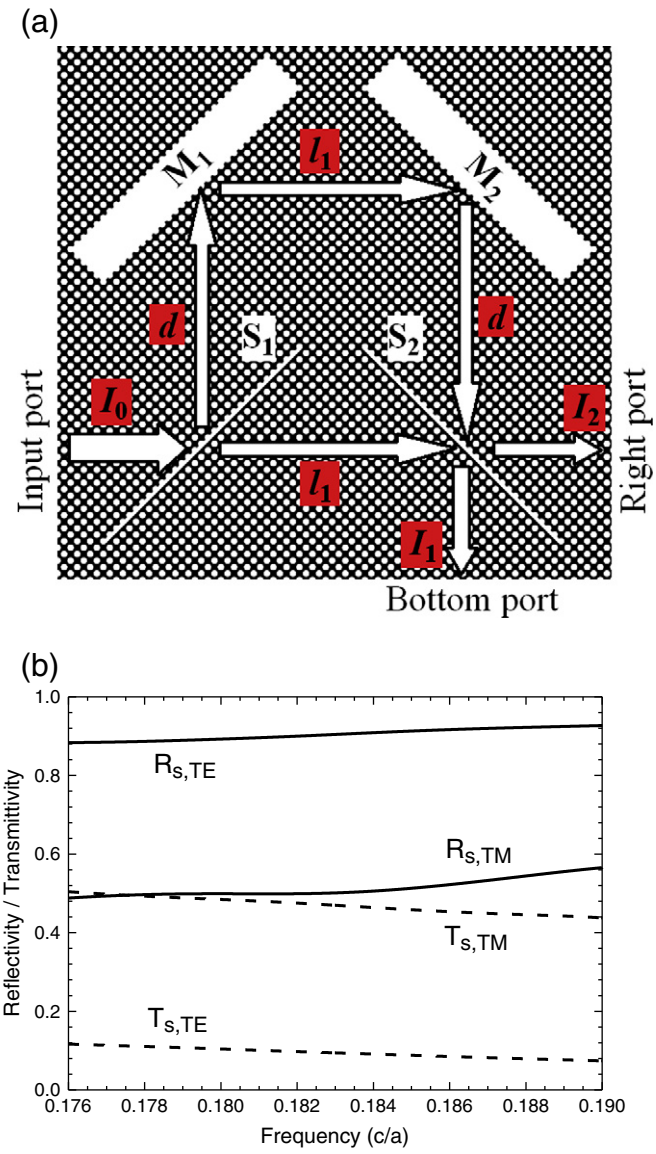


**Fig. 2.** (a) Structure of the SMZI consisting of two beam splitters ($S_1$ and $S_2$) and two mirrors ($M_1$ and $M_2$). The arrows indicate the propagation directions of the self-collimated light beams. (b) Polarization-dependent reflectivity ($R_s$) and transmittivity ($T_s$) of one beam splitter in the common SC frequency range.

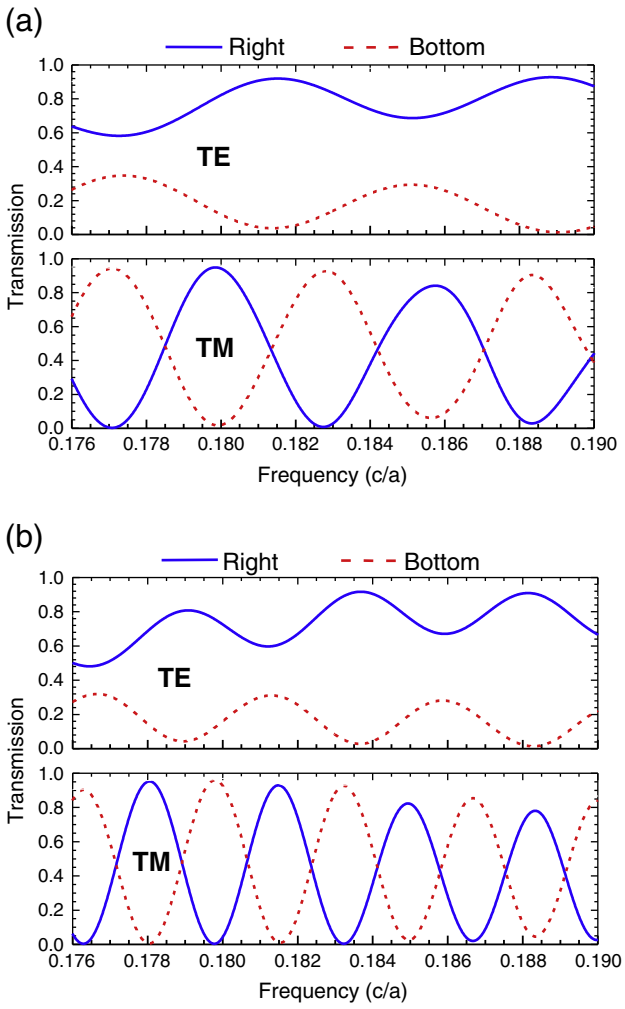


**Fig. 3.** FDTD simulated transmission spectra of the SMZI for TE and TM modes at the right (blue solid lines) and bottom (red dash lines) output ports when (a) $d = 15\sqrt{2}a$ and (b) $d = 25\sqrt{2}a$.

bottom and right transmissions have the largest amplitude of 1 and are in the same range [0, 1]. When $R_s \neq 0.5$ (i.e., $4R_sT_s<1$), however, their amplitudes diminish to less than 1 and their ranges separate. As a result, the right transmission has higher vertical position than the bottom transmission.

To verify the theoretical analyses aforementioned, the transmission spectra of the SMZI are simulated numerically with the FDTD method. A Gaussian optical pulse is launched at the input port. The input power ($I_0$), bottom and right output power ($I_1$ and $I_2$) are monitored with three power monitors respectively. The transmission spectra when $d = 15\sqrt{2}a$ or $d = 25\sqrt{2}a$ are shown in Fig. 3(a) and (b), respectively. The bottom and right transmission curves are plotted as red dash lines and blue solid lines, respectively. For TM modes, both the bottom and right transmissions are approximately in the range [0, 1]. For TE modes, however, they separate and locate approximately in the range [0, 0.36] and [0.64, 1] respectively. Considering the polarization dependent reflectivity and transmittivity values of the splitters in Fig. 2(b), the simulated results agree very well with the theoretical prediction.

In addition, as can be seen in Fig. 3, the ratio of the peak spacings for TE and TM transmission spectra is about 4:3 for the same SMZI size, which agrees well with the ratio of the effective indices for two polarizations ($n_{e,TE}:n_{e,TM}\approx 3:4$) [14]. The peak spacings decrease when the length difference $2d$ between the two light paths increases.

## 4. Design of PBS based on SMZI

We had proposed the polarization peak matching (PPM) method and applied it to design a polarization-independent drop filters based on a PC self-collimation ring resonator [14]. Now we utilize the PPM method again to design a PBS based on a SMZI.

As shown in Fig. 3, TE and TM transmission spectra are quite different in terms of vertical range and horizontal peak spacing. On the other hand, both TE and TM peak frequencies shift when the path length difference $2d$ changes. Considering these two factors, we found that a SMZI can work as a PBS if a bottom transmission peak for TM modes has the same frequency as a right transmission peak for TE modes, which is so-called polarization peak matching (PPM). Here, it is worth noticing that the splitters must possess 1:1 splitting ratio for TM modes. According to Chen et al. [14], it is not difficult to find out some PPM cases by changing the path length difference. With the FDTD method, we simulated the transmission spectra for TM and TE

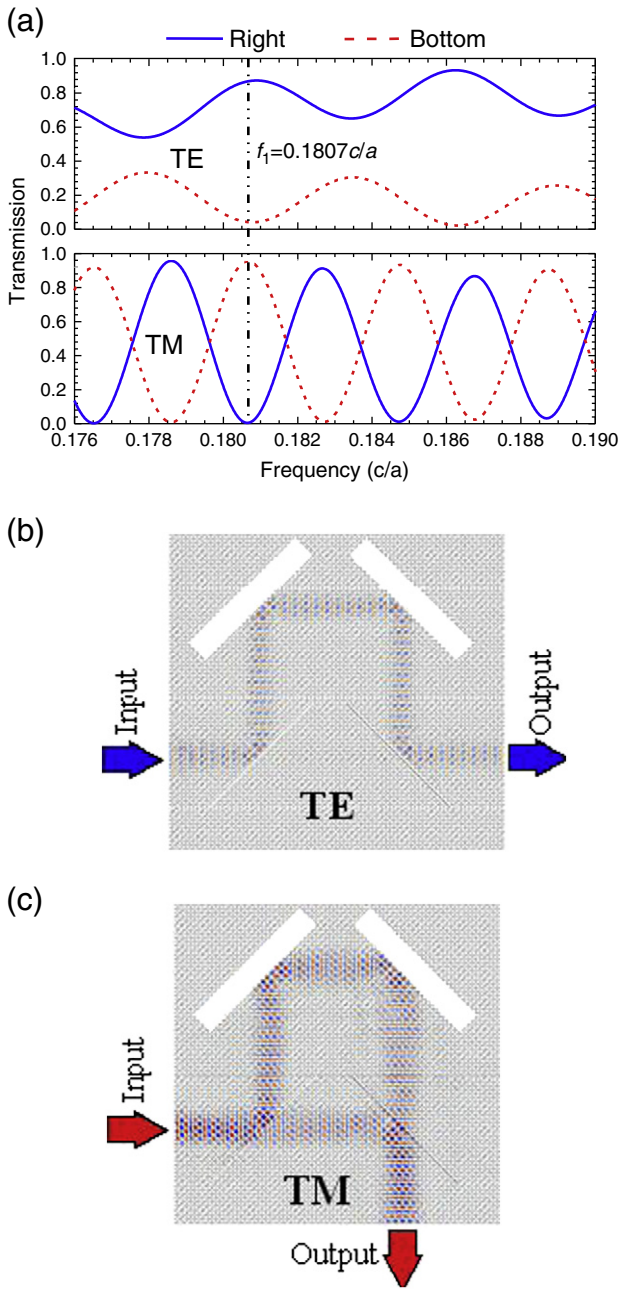


**Fig. 4.** (a) FDTD simulated right transmission (blue solid lines) and bottom transmission (red dash lines) for both TE and TM polarizations when $d = 21\sqrt{2}a$. Notice PPM happens at $f_1 = 0.1807c/a$. FDTD simulated magnetic-field distribution for TE polarization (b) and electric-field distribution for TM polarization (c) for input light at $f_1 = 0.1807c/a$.

polarizations by scanning the values of $d$ from $10\sqrt{2}a$ to $d = 25\sqrt{2}a$, with step length of $\sqrt{2}a$. The results show that there exist several PPM cases. The best PPM happens when $d = 21\sqrt{2}a$, in which a bottom TM transmission peak matches well with a right TE transmission peak at $f_1 = 0.1807c/a$(corresponding wavelength in vacuum $\lambda_1 = c/f_1 = 5.534a$), as shown in Fig. 4(a). The field distribution patterns of the SC light at $f_1$ for TE and TM modes were also simulated as shown in Fig. 4(b) and (c), respectively. It can be seen clearly that TE light goes out from the right port, while TM light goes out from the bottom port. The polarization extinction ratios (PERs) for TE and TM modes are $PER_{TE} = 10\lg(I_{2,TE}/I_{1,TE})13.2\text{dB}$ and $PER_{TM} = 10\lg(I_{1,TM}/I_{2,TM})23.2\text{dB}$, respectively. Such a PBS can be designed to operate at any frequencies according to the scaling law for PCs. For example, if the lattice constant $a$ and air hole radius $r$ are equal to 280.1 nm and 92.4 nm respectively, the operating wavelength is equal to 1550 nm.

## 5. Conclusions

In conclusion, we designed a SMZI interferometer in a hole-type silicon photonic crystal which can work for both TE and TM polarizations in the common SC frequency window. Then polarization peak matching method was applied to realize a PBS based on a SMZI. Its performance was evaluated with FDTD simulation technique and good agreements are obtained between the simulation and the theory. Due to its novel operating principle based on the polarization dependence of self-collimated light interference, this PBS can have high PERs. It can work at any frequencies by scaling lattice constant and air hole radius simultaneously for PCs. For the operating wavelength at 1550 nm, the dimensions of this PBS are about several microns. So the SMZI-based PBS may play an important role in high-density photonic integrated circuits. Although the PBS is designed based on 2D PCs, it may be designed based on more practical PC slabs where TE-like and TM-like guided modes exist [21], which belongs to our future work.

## Acknowledgements

This work was supported in part by the Natural Science Foundation of Fujian Province of China under Grant no. 2009 J01012 and by the Research Projects of Science and Technology of Fujian Education Office of China under Grant no. JA08183.

## References

[1] H. Kosaka, T. Kawashima, A. Tomita, M. Notomi, T. Tamamura, T. Sato, S. Kawakami, Appl. Phys. Lett. 74 (1999) 1212.
[2] J. Witzens, M. Lončar, A. Scherer, IEEE J. Sel. Top. Quantum Electron. 8 (2002) 1246.
[3] L. Wu, M. Mazilu, T.F. Krauss, J. Lightwave Technol. 21 (2003) 561.
[4] X. Yu, S. Fan, Appl. Phys. Lett. 83 (2003) 3251.
[5] P.T. Pakich, M.S. Dahlem, S. Tandon, M. Ibanescu, M. Soljacic, G.S. Petrich, J.D. Johnnopolos, L.A. Kolodziejski, E.P. Ippen, Nat. Mater. 5 (2006) 93.
[6] D.W. Prather, S. Shi, J. Murakowski, G.J. Schneider, A. Sharkawy, C. Chen, B. Miao, R. Martin, J. Phys. D 40 (2007) 2635.
[7] D. Zhao, C. Zhou, Q. Gong, X. Jiang, J. Phys. D Appl. Phys. 41 (2008) 15108.
[8] D. Zhao, J. Zhang, P. Yao, X. Jiang, X. Chen, Appl. Phys. Lett. 90 (2007) 231114.
[9] V. Zabelin, L.A. Dunbar, N.L. Thomas, R. Houdré, Opt. Lett. 32 (2007) 530.
[10] X.P. Shen, K. Han, F. Yuan, H.P. Li, Z.Y. Wang, Q. Zhong, Chin. Phys. Lett. 25 (2008) 4288.
[11] T.-T. Kim, S.-G. Lee, H.Y. Park, J.-E. Kim, C.-S. Kee, Opt. Express 18 (2010) 5384.
[12] H.M. Nguyen, M.A. Dundar, R.W. van der Heijden, E.W.J.M. van der Drift, H.W.M. Salemink, S. Rogge, J. Caro, Opt. Express 18 (2010) 6437.
[13] J. Hou, D. Gao, H. Wua, Z. Zhou, Opt. Commun. 282 (2009) 3172.
[14] X. Chen, Z. Qiang, D. Zhao, H. Li, Y. Qiu, W. Yang, W. Zhou, Opt. Express 17 (2009) 19808.
[15] T. Liu, A.R. Zakharian, M. Fallahi, J.V. Moloney, M. Mansuripur, IEEE Photon Techol. Lett. 17 (2005) 1435.
[16] P. Pottier, S. Mastroiacovo, R.M. De La Rue, Opt. Express 14 (2006) 5617.
[17] E. Schonbrun, Q. Wu, W. Park, T. Yamashita, C.J. Summers, Opt. Lett. 31 (2006) 3104.
[18] W. Zheng, M. Xing, G. Ren, S.G. Johnson, W. Zhou, W. Chen, L. Chen, Opt. Express 17 (2009) 8657.
[19] P. Yeh, J. Opt. Soc. Am. 69 (1979) 742.
[20] B.E.A. Saleh, M.C. Teich, Fundamentals of Photonics, A Wiley-Interscience Publication, New York, 1991.
[21] S.G. Johnson, S. Fan, P.R. Villeneuve, J.D. Joannopoulos, Phys. Rev. B 60 (1999) 5751.